

SPHERICAL LOUDSPEAKER ARRAY MODELING AND CONTROL USING DIFFERENT BASIS FUNCTION REPRESENTATIONS

Dima Khaykin and Boaz Rafaely

Department of Electrical and Computer Engineering
Ben-Gurion University of the Negev
Beer-Sheva 84105, Israel
{khaykin,br}@ee.bgu.ac.il

ABSTRACT

A potential use of a spherical loudspeaker array for producing arbitrary radiation patterns has recently been studied. Different control strategies were developed and proposed for this goal. This work attempts to make a connection between two popular control strategies: the loudspeaker units input signals and the gains of spherical harmonics directivities. These control strategies make use of two sets of basis functions: caps' velocity and spherical harmonics, respectively, that fully span the radiation subspace. A new set of basis functions that spans the same subspace as spherical harmonics and cap velocity is developed using a singular-value decomposition and shown to be of finite order, unlike the spherical harmonics set. These new basis functions provide an indication of the way the spherical loudspeaker array produces the spherical harmonics modes of different orders. Control strategy based on these new basis functions is formulated and its performance compared to already mentioned strategies by producing quiet zones as an application of active sound control. In addition, the ability of this new control strategy to design various radiation patterns analytically, rather than by numerical optimization, is discussed and demonstrated.

1. INTRODUCTION

The study of spherical loudspeaker arrays has been an active area of research in recent years. Due to its compact design, which usually consists of a set of loudspeakers mounted around the surface of a sphere, it can be used as an effective device for synthesis of a sound field. Different models of the spherical loudspeaker array have been developed and studied. A model of L spherical caps positioned on the sphere surface with each imposing a surface radial velocity at the sphere surface segment it covers [1, 2], has been considered as a good approximation to a real spherical loudspeaker array with L loudspeakers positioned around the sphere surface. Using a spherical loudspeaker array as a multi-channel source and controlling each loudspeaker unit individually, complex sound radiation patterns can be achieved. The need to design the radiated sound field by controlling the loudspeaker units in a multi-channel system framework is common in applications such as music synthesis, active control of sound, and room acoustics. Various control strategies of loudspeaker units were proposed and discussed in recent years.

The aim of this paper is to provide analysis of the advantages and disadvantages of using different types of representations for the modeling and control of sound radiation with a loudspeaker array. Due to the spherical design of the loudspeaker array, spherical harmonics are the most natural and common basis

functions for controlling the array radiation pattern. As part of the solution of the Helmholtz equation in spherical coordinates, spherical harmonics form a natural basis for representation of sound source directivity and provide full analytical analysis of the sound field and sound system. Thus, a simple and effective way to produce arbitrary radiation patterns is to control the amplitudes of these spherical harmonics functions, representing, for example, array surface velocity or the produced far-field pressure. However, to achieve arbitrary radiation patterns, full control over amplitudes of an infinite number of spherical harmonics is required. Because the number of loudspeaker units in an array is limited in practice, the number of spherical harmonics functions that can be controlled is also limited. Hence, harmonics of the higher orders, which cannot be controlled directly, may produce errors in the radiated sound field. Control of a finite set of spherical harmonics without considering the effect of the radiated high-order harmonics, may produce inferior control of the array output, as recently presented in the application of the array for active control of sound [3].

Control over the velocities of the caps, or the loudspeaker units input signals, may be considered a more direct and practical approach as it uses the physical input signals of the multi-channel system directly. In their work, Aviziens et al. [4] implemented such a strategy to produce radiation patterns with a spherical loudspeaker array consisting of 120 elements. In addition, the rationale behind this approach is that the control strategy in the space domain, rather than the spherical harmonics, does not require any assumptions concerning the spherical harmonics order. In other words, this control strategy does not require a basis of an infinite dimension, but makes use of a finite number of functions, representing cap velocity or loudspeaker inputs. However, the drawback of this strategy is that in most cases only a numerical analysis can be employed, as the basis functions in this case cannot be readily used to analytically represent other forms of sound fields, such as a plane wave or a point source. This is in contrast to the use of spherical harmonics basis functions, where plane waves and point sources can be represented analytically in a straight-forward manner.

This paper proposes an intermediate basis function, combining spherical harmonics functions and cap velocity functions. By performing singular-value decomposition (SVD) of the transfer matrix relating the spherical Fourier coefficients of the (continuous) radial surface velocity to the vector of cap velocities, we form a new set of basis functions that spans the same subspace as the cap velocities functions and the spherical harmonics functions for the spherical array. We show that this new set of basis functions is closely related to spherical harmonics; however, it

is finite, and hence has an advantage over the spherical harmonics basis set. In addition, the paper presents an investigation of the use of the various basis functions in the application of local active control of sound. Zones of quiet are generated using the mentioned control strategies and the results are compared and discussed.

2. SOUND RADIATION FROM SPHERICAL SOURCES

This section introduces two spherical sources that are considered throughout this paper:

S1. A sphere with a continuous radial velocity distribution on its surface.

S2. A rigid sphere with L spherical caps positioned on its surface at locations (θ_l, ϕ_l) , each imposing a constant radial surface velocity of v_l , $l = 1, \dots, L$, at the surface segment they cover.

The acoustic pressure defined on the surface of a sphere is denoted by $p(k, r, \theta, \phi)$, where (θ, ϕ) with a sphere radius r , combined to define the standard spherical coordinates [5], and k is the wavenumber.

The sound field produced by a spherical source having coefficients of radial surface velocity u_{nm} is given by [6]:

$$p(k, r, \theta, \phi) = i\rho_0 c \sum_{n=0}^{\infty} \sum_{m=-n}^n \frac{h_n(kr)}{h'_n(kr_0)} u_{nm}(k, r_0) \times Y_n^m(\theta, \phi), \quad (1)$$

where $h_n(kr)$ is the spherical Hankel function of first kind and order n , $h'_n(\cdot)$ represents derivative, and $Y_n^m(\theta, \phi)$ are the spherical harmonics of order n and degree m [5]. r_0 is the radius of the sphere, c is the speed of sound, and ρ_0 is the density of the air. By defining

$$g_n = \frac{4\pi^2}{2n+1} [P_{n-1}(\cos \alpha) - P_{n+1}(\cos \alpha)], \quad (2)$$

where $P_{n-1}(\cdot)$ is the Legendre polynomial and α is the aperture angle of the cap, the spherical Fourier coefficients of the radial surface velocity are related to the caps' velocity of S2 by [2]

$$u_{nm}(k, r_0) = g_n \sum_{l=1}^L v_l(k, r_0) Y_n^{m*}(\theta_l, \phi_l). \quad (3)$$

Equations (1) and (3) provide the relation between the acoustic pressure and the caps' velocity, forming the model for source S2 that can be used to predict the acoustic pressure field, given the radial velocity of each cap. It is worth noting that with L spherical caps, only L spherical harmonics in u_{nm} can be controlled, defined in the range $n \leq N$, $-n \leq m \leq n$, with N satisfying

$$(N+1)^2 \leq L. \quad (4)$$

Hence, by truncating the sum in (1), it can be re-written in a matrix form

$$\mathbf{p} = \mathbf{A}\mathbf{u}. \quad (5)$$

where \mathbf{p} is the vector of the desired acoustic pressure samples, given by $\mathbf{p} = [p_1, p_2, \dots, p_Q]^T$, with $p_q = p(k, r_q, \theta_q, \phi_q)$,

$Q \times (N+1)^2$ matrix \mathbf{A} is defined by the elements A_{qj} and $(N+1)^2 \times 1$ vector \mathbf{u} defined by the elements u_j , given by:

$$\begin{aligned} A_{qj} &= i\rho_0 c \frac{h_n(kr)}{h'_n(kr_0)} Y_n^m(\theta_q, \phi_q) \\ u_j &= u_{nm} \\ j &= n^2 + n + m + 1, n \leq N, -n \leq m \leq n, \end{aligned} \quad (6)$$

In the same way, the relation between the acoustic pressure and the caps' velocity can be written. Let us re-write (3) as:

$$\mathbf{u} = \mathbf{G}\mathbf{Y}^H \mathbf{v}, \quad (7)$$

where $\mathbf{v} = [v_1, v_2, \dots, v_L]$ represents a vector of the radial caps' velocity, the matrix \mathbf{Y} is of dimensions $L \times (N+1)^2$ and is defined by elements Y_{lj} , given by $Y_{lj} = Y_n^m(\theta_l, \phi_l)$, where j is defined in (6) and $(N+1)^2 \times (N+1)^2$ matrix $\mathbf{G} = \text{diag}[g_0, g_1, g_1, g_1, \dots, g_N]$. Now, by substituting (7) in (5) we get the final expression

$$\mathbf{p} = \mathbf{A}\mathbf{G}\mathbf{Y}^H \mathbf{v}. \quad (8)$$

In [2], Rafaely showed that for order-limited radial velocity, sources S1 and S2 can be used to produce the same acoustic pressure field on the assumption that (4) stands. Therefore, one may prefer the use of source S1 due to its relative simplicity and ease of analytical analysis.

3. ACTIVE CONTROL OF SOUND

Active control of sound is achieved by superimposing the primary sound field p_p with the secondary sound field p_s , produced by an acoustic source. As an application, we make an attempt to produce quiet zones by using two control strategies over spherical loudspeaker arrays: control over the gains of spherical harmonics directivities, and control over the velocities of the spherical caps.

The first strategy makes use of a least-squares solution as a numerical optimization over \mathbf{u} :

$$\mathbf{u} = \mathbf{A}^\dagger \mathbf{p} \quad (9)$$

where $(\cdot)^\dagger$ represents the pseudo-inverse operation.

The second control strategy uses the same least-squares solution as a numerical optimization, but over \mathbf{v} :

$$\mathbf{v} = (\mathbf{A}\mathbf{G}\mathbf{Y}^H)^\dagger \mathbf{p}. \quad (10)$$

The components of vector \mathbf{p} are the samples of a given sound field p_s .

As mentioned at the end of previous section, if the required radial velocity is order-limited such that (4) stands, the two aforementioned control strategies provide identical results. However, in the case that the desired acoustic pressure is more complicated and requires a radial velocity of infinite order or at least such that (4) does not stand, the second strategy, based on the velocity caps' optimization, is a preferred strategy, since it makes no assumption on the order of harmonics that are controlled by the spherical array [3].

The following simulation example aims to compare the performance of the two aforementioned control strategies. The experiment was performed using a spherical source of radius $r_0 = 0.1$ meters with $L = 84$ uniformly-distributed caps on

its surface. Since the source has 84 degrees of freedom, using the first control strategy we can control only harmonics up to order $N = 8$ and the harmonics of higher order are neglected. In the second case, harmonics up to $N = 40$ are incorporated to represent “infinite” order.

The primary sound field p_p is composed of 20 plane-waves with unit magnitude, frequency of 1000 Hz, and random phases and arrival directions. Two control strategies were implemented to minimize the total pressure p_t , which is the superposition of the primary and secondary sound fields, i.e., $p_t = p_p + p_s$, at a set of locations in the range $r \in [0.2, 0.3]$, $\theta = 90^\circ$, and $\phi \in [0^\circ, 360^\circ)$. Attenuation levels, calculated as $20 \log_{10} \left(\frac{p_t}{p_p} \right)$, are presented in Fig. 1, and the desired quiet zone is defined by dashed lines. Fig. 1(a) presents the result achieved by control over the spherical Fourier coefficients of the radial surface velocity, i.e., using (9), when harmonics up to order $N = 8$ are used. Fig. 1(b) shows the attenuation levels achieved by the second control strategy, based on an optimization over the caps’ velocity directly, i.e., using (10). Comparing these results shows that the caps’ velocity strategy is a preferred control strategy in this case.

To make an attempt to connect the spherical harmonics and caps’ velocity control strategies, in the next section we develop a new basis function that spans the same subspace as spherical harmonics and caps’ velocity, but forms a finite set and is closely related to spherical harmonics.

4. A RELATION BETWEEN SPHERICAL HARMONICS AND CAPS’ VELOCITY

In this development we make no assumption on the maximum order of radial velocity, hence order N represents “infinity” throughout this section. However, the number of spherical caps L is assumed to be finite. Let us perform the singular-value decomposition (SVD) of the transfer matrix relating the spherical Fourier coefficients of radial surface velocity to caps’ velocity from (7):

$$\mathbf{G}\mathbf{Y}^H = \mathbf{S}\mathbf{\Sigma}\mathbf{R}^H \quad (11)$$

where $(N+1)^2 \times (N+1)^2$ matrix \mathbf{S} and $L \times L$ matrix \mathbf{R} comprise the left and right singular vectors, and matrix $\mathbf{\Sigma}$ has L singular values and $(N+1)^2 - L$ zero rows. By substituting (11) in (7) and multiplying from left by \mathbf{S}^H we get

$$\mathbf{S}^H \mathbf{u} = \mathbf{\Sigma} \mathbf{R}^H \mathbf{v}. \quad (12)$$

Let us define two terms: $\mathbf{a} \equiv \mathbf{R}^H \mathbf{v}$ and $\mathbf{b} \equiv \mathbf{S}^H \mathbf{u}$. By using the unitary property of \mathbf{S} and \mathbf{R} , respectively, we get:

$$\mathbf{v} = \mathbf{R} \mathbf{a}, \quad (13)$$

$$\mathbf{u} = \mathbf{S} \mathbf{b}. \quad (14)$$

The elements of these vectors can be written as

$$v_l = \sum_{p=1}^L R_{lp} a_p \quad (15)$$

$$u_j = \sum_{s=1}^{(N+1)^2} S_{js} b_s. \quad (16)$$

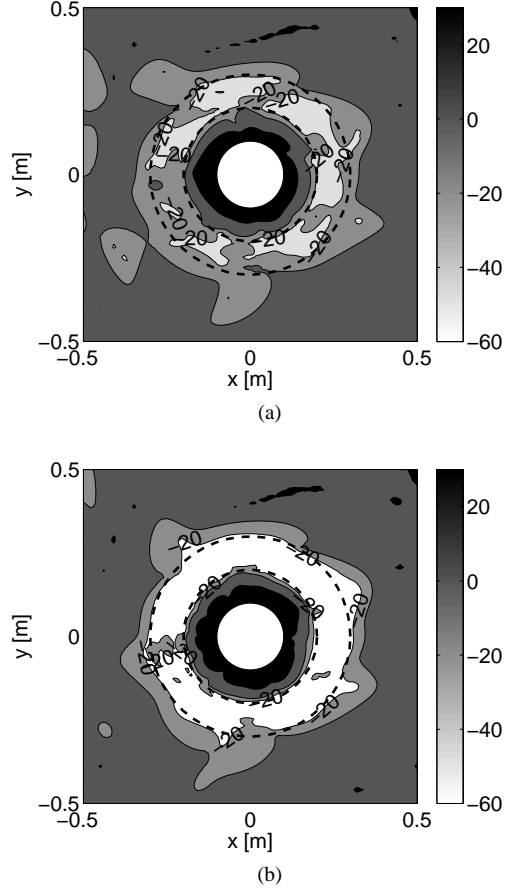


Figure 1: Magnitude, in decibels, of the acoustic pressure produced by a spherical source with $L = 84$ caps, designed to create a quiet zone at a range of points around $r \in [0.2, 0.3]$, $\theta = 90^\circ$, and $\phi \in [0^\circ, 360^\circ)$, with control strategy based on (a) spherical Fourier coefficients of radial surface velocity \mathbf{u} , (b) caps’ velocity \mathbf{v} .

Now, the continuous velocity function $v(\theta, \phi)$ can be calculated in two ways. Using cap velocity basis functions $\Pi(\Theta_l)$,

$$v(\theta, \phi) = \sum_{l=1}^L v_l \Pi(\Theta_l), \quad (17)$$

where $\Pi(\Theta_l)$ and Θ_l are defined as

$$\Pi(\Theta_l) = \begin{cases} 1, & \Theta_l \leq \alpha \\ 0, & \text{elsewhere} \end{cases}, \quad (18)$$

$$\cos \Theta_l = \cos \theta \cos \theta_l + \cos(\phi - \phi_l) \sin \theta \sin \theta_l, \quad (19)$$

or using spherical harmonics,

$$v(\theta, \phi) = \sum_{j=1}^{(N+1)^2} u_j Y_j(\theta, \phi). \quad (20)$$

By substituting (15) in (17) we get

$$v(\theta, \phi) = \sum_{l=1}^L \sum_{p=1}^L R_{lp} a_p \Pi(\Theta_l), \quad (21)$$

and by changing the order of sums, new basis functions $\Psi_p(\theta, \phi)$ are obtained

$$v(\theta, \phi) = \sum_{p=1}^L a_p \Psi_p(\theta, \phi), \quad (22)$$

$$\Psi_p(\theta, \phi) = \sum_{l=1}^L R_{lp} \Pi(\Theta_l). \quad (23)$$

In the same way, by substituting (16) into (20) we can obtain another set of basis functions

$$v(\theta, \phi) = \sum_{s=1}^{(N+1)^2} b_s \Phi_s(\theta, \phi), \quad (24)$$

$$\Phi_s(\theta, \phi) = \sum_{j=1}^{(N+1)^2} S_{js} Y_j(\theta, \phi). \quad (25)$$

Actually, since $\mathbf{b} = \Sigma \mathbf{a}$, $\Psi_p(\theta, \phi)$ is equal to $\Phi_s(\theta, \phi)$ up to a constant singular value of Σ . Since Σ has zero rows, the number of new basis functions and related coefficients is finite and equal to L , the number of singular values, meaning the sum in (24) is up to L or equivalent, and only the first L columns of matrix \mathbf{S} are relevant. Hence, this set has a finite order compared to the spherical harmonics basis set.

5. NEW BASIS FUNCTIONS ANALYSIS AND IMPLEMENTATION

In this section, the new basis functions are illustrated to visually demonstrate the relation between spherical harmonics and caps' velocity functions. A new control strategy, using the new basis functions, is formulated, and its performance compared to aforementioned control strategies. In addition, the advantages of implementation of the new basis functions are discussed.

In this experiment we used $N = 40$ to represent "infinite" order and 12 caps positioned on the sphere. Figure 2 shows the first 12 basis functions $\Phi_s(\theta, \phi)$. This figure effectively demonstrates the connection between the caps' velocity and spherical harmonics. As can be seen in Fig. 2, $\Phi_s(\theta, \phi)$ functions are closely related to spherical harmonics and can be divided into the same groups as spherical harmonics: $\Phi_1(\theta, \phi)$, $\Phi_{2-4}(\theta, \phi)$, $\Phi_{5-9}(\theta, \phi)$, $\Phi_{10-12}(\theta, \phi)$. By examining $\Phi_s(\theta, \phi)$, one can perceive an indication of how the spherical source caps vibrate to make an attempt to produce the radiation pattern of spherical harmonics shapes. For example, to produce spherical harmonics of order $n = 0$ (monopole), all the caps oscillate coherently as demonstrated by $\Phi_1(\theta, \phi)$. The second group, $\Phi_{2-4}(\theta, \phi)$, are related to spherical harmonics of order $n = 1$, as they produce dipoles. According to $\Phi_{5-9}(\theta, \phi)$, the sphere caps are related to spherical harmonics of order $n = 2$, which look like quadrupoles. The rest, $\Phi_{10-12}(\theta, \phi)$, are related to spherical harmonics of order $n = 3$.

A new control strategy, using the new basis functions, can now be formulated. This control strategy benefits from finite order and makes no assumption on the order of spherical harmonics that can be controlled. Hence, the ability to produce a complex sound field may be greater than with the strategy based on spherical harmonics.

By substituting (14) into (5) we get the relation between the acoustic pressure and new coefficients

$$\mathbf{p} = \mathbf{A} \mathbf{S} \mathbf{b}. \quad (26)$$

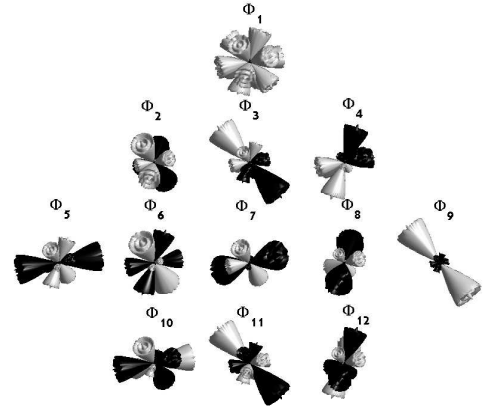


Figure 2: First 12 basis functions $\Phi_s(\theta, \phi)$ developed in (25).

Since no assumption is made on the order of spherical harmonics, N , it can be assumed "infinite". However, the number of coefficients in vector \mathbf{b} is finite; hence it has to be equal to the number of caps L . Coefficient \mathbf{b} can be calculated by using the same least square solution as used in (9) and (10)

$$\mathbf{b} = (\mathbf{A} \mathbf{S})^\dagger \mathbf{p}. \quad (27)$$

To compare the performance of this new control strategy with the two control strategies mentioned before, the same experimental study that was described in Section 3 was performed in this case. The order of harmonics was set to $N = 40$, to represent the "infinite" order, and the number of caps was, as in the previous experiment, $L = 84$. Since the source has 84 degrees of freedom, the maximum components of vector \mathbf{b} are also 84, hence only 84 columns in matrix \mathbf{S} are relevant. Therefore, matrix \mathbf{S} is now of dimensions $(N+1)^2 \times L$.

Figure 3 shows the attenuation levels achieved by the new control strategy. It can be noticed that the new strategy outperforms the spherical harmonics strategy and achieves the same results as the caps' velocity strategy.

This experiment showed the advantage of using new basis functions compared with a spherical harmonics set. To emphasize the advantage over the caps' velocity basis functions, we provide a simple example. To achieve most radiation patterns by controlling the caps' velocity directly, only numerical optimization can be implemented. In contrast to this approach, use of new basis functions can provide a simpler way to realize these patterns. Let us consider a cardioid radiation pattern. By combining Φ_1 and one of the basis functions (or linear combination of them) demonstrated in the second row in Fig. 2, i.e., Φ_{2-4} , we can easily realize cardioid radiation pattern. For example, let us add Φ_1 and Φ_3 , i.e., set the components of vector \mathbf{b} as follows

$$\mathbf{b} = [1, 0, 1, 0, \dots, 0]^T. \quad (28)$$

Figure 4 shows the result of this sum. The radiation pattern can be achieved now by substituting (28) in (26). The experiment was performed using a spherical source of radius $r_0 = 0.1$ meters with $L = 12$ uniformly-distributed caps on its surface. Figure 5 shows the radiation pattern, i.e., sound pressure as measured at $r = 0.5$ and frequency $f = 1000$ Hz. The pattern was found to be very similar to the cardioid pattern as planned.

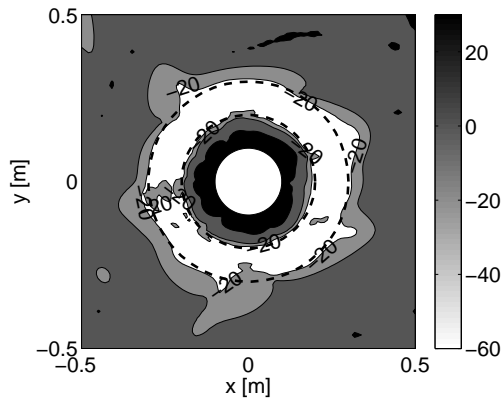


Figure 3: Magnitude, in decibels, of the acoustic pressure produced by a spherical source with $L = 84$ caps designed to create a quiet zone at a range of points around $r \in [0.2, 0.3]$, $\theta = 90^\circ$, and $\phi \in [0^\circ, 360^\circ)$, with control strategy based on the new set of basis functions developed in Sec. 4.

One can notice that the radiation pattern is smoothed (consists of low-order spherical harmonics only), despite being realized by spherical caps, which are shown to also produce high-order harmonics. The reason for this is the $\frac{h_n(kr)}{h_n(kr_0)}$ term that operates as a low order filter. For extended discussion, the reader is referred to [2].

6. SUMMARY AND CONCLUSIONS

In this paper, we developed new basis functions that relate to spherical harmonics and caps' velocity. These new basis functions illustrate how the spherical source produces modes that are related to the spherical harmonics modes. In addition, control strategy was presented based on these new basis functions. This set of basis functions is finite; hence the ability to produce a complex sound field may be greater than the strategy based on spherical harmonics. This was confirmed by simulation studies. Analytical solution of the realization of radiation patterns was shown to be an advantage over the control strategy based on loudspeaker units input signals, which requires numerical optimization. As an example, cardioid radiation pattern was realized using the new set of basis functions.

7. ACKNOWLEDGMENT

This work was supported in part by the Ministry of Industry and Trade (grant no. 40161).

8. REFERENCES

- [1] F. Zotter, A. Sontacchi, and R. Holdrich, "Modeling a spherical loudspeaker system as multipole source," *FORTSCHRITTE DER AKUSTIK*, vol. 33, no. 1, p. 221, 2007.
- [2] B. Rafaely, "Spherical loudspeaker array for local active control of sound," *J. Acoust. Soc. Am.*, vol. 125, no. 5, pp. 3006–3017, May 2009.

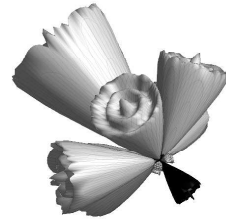


Figure 4: Sum of $\Phi_1(\theta, \phi)$ and $\Phi_3(\theta, \phi)$ functions.

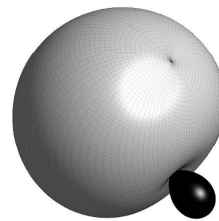


Figure 5: Cardioid pressure radiation pattern realized by sum of $\Phi_1(\theta, \phi)$ and $\Phi_3(\theta, \phi)$ functions.

- [3] D. Lederman and B. Rafaely, "Spherical loudspeaker array modeling for active control of sound," in *The 2009 International Symposium on Active Control of Sound and Vibration (ACTIVE 2009)*, Ottawa, Canada, August 2009.
- [4] R. Avizienis, A. Freed, P. Kassakian, and D. Wessel, "A compact 120 independent element spherical loudspeaker array with programmable radiation patterns," in *Proc. 120th AES-Convention, Paris, 2006*.
- [5] G. B. Arfken and H. J. Weber, *Mathematical Methods for Physicists*, 6th ed. Oxford: Elsevier Academic Press, 2005.
- [6] E. G. Williams, *Fourier Acoustics: Sound Radiation and Nearfield Acoustical Holography*. New York, NY: Academic Press, 1999.